



Cite this: *Nanoscale*, 2017, **9**, 16143

Received 6th September 2017,
 Accepted 12th October 2017

DOI: 10.1039/c7nr06661a

rsc.li/nanoscale

Multi-exciton emission from solitary dopant states of carbon nanotubes†

Xuedan Ma,^{†a} Nicolai F. Hartmann,^{†a} Kirill A. Velizhanin,^{†*b} Jon K. S. Baldwin,^{†a} Lyudmyla Adamska,^b Sergei Tretiak,^{†a,b} Stephen K. Doorn^{†a} and Han Htoon^{†*a}

By separating the photons from slow and fast decays of single and multi-exciton states in a time gated 2nd order photon correlation experiment, we show that solitary oxygen dopant states of single-walled carbon nanotubes (SWCNTs) allow emission of photon pairs with efficiencies as high as 44% of single exciton emission. Our pump dependent time resolved photoluminescence (PL) studies further reveal diffusion-limited exciton–exciton annihilation as the key process that limits the emission of multi-excitons at high pump fluences. We further postulate that creation of additional permanent exciton quenching sites occurring under intense laser irradiation leads to permanent PL quenching. With this work, we bring out multi-excitonic processes of solitary dopant states as a new area to be explored for potential applications in lasing and entangled photon generation.

Introduction

Doping of single wall carbon nanotubes (SWCNTs) *via* covalent attachment of various chemical functional groups^{1–6} such as ether/epoxide,^{1,5} alkyl⁴ and aryl⁶ species has been rapidly emerging as an effective means for enhancing emissive properties of SWCNTs and introducing new functionalities. Specifically, dramatic enhancement of emission efficiency, realized *via* localization of 1D excitons to 0D states capable of emitting PL at an energy 130 to 300 meV below the band-edge,^{5–7} brings new promise for SWCNT-based bio-imaging,¹ light emitting devices and lasers.^{7,8} Furthermore, recent demonstrations of room temperature single photon

generation in oxygen⁹ and aryl¹⁰ functionalized SWCNTs establishes solitary dopant states as a new type of quantum light source. Moreover, development of a solid-state doping approach, in which the solitary oxygen dopant states are introduced *via* a simple deposition of SiO₂ or Al₂O₃ thin films,¹¹ makes the doped nanotubes compatible with existing micro-electronic technologies^{12–16} and opens a path toward development of photonic integrated circuits.¹⁷

Although recent studies have brought significant new understanding of the electronic structure,⁵ non-linear optical properties,^{5,8} and PL fluctuation behaviors of doped SWCNTs,^{9,18} many critical photophysical processes remain virtually unexplored. Among these, questions such as whether a solitary dopant site can accommodate multiple excitons as in the case of quantum dots,^{19,20} how efficiently these multiple excitons can recombine radiatively, and how these excitons interact with one another, are particularly important. While formation and recombination of multiple exciton states is not so desirable for single photon generation,^{21–25} understanding and control of these processes could enable new functionalities such as generation of entangled photon pairs^{26,27} and optical amplification. Some indications of multi-excitons were observed in our recent studies.

Specifically, while some oxygen doped tubes exhibit near complete photon antibunching⁹ characterized by a vanishing peak at zero time delay (*i.e.* center peak area $g^{(2)}(0) \cong 0$) in second order photon correlation plots, some degree of photon bunching with a normalized center peak area ($R = g^{(2)}(0)/$ average area of side peaks far from the zero time delay, see ESI 1†) in the range of 0.25 to 0.5 was observed in a significant number of oxygen doped tubes. For example, at 200 K, 60% of ~40 CNTs show antibunching ($R < 0.5$) and ~20% exhibit R between 0.25 and 0.5, indicating that some doped tubes emit more than one photon in one excitation cycle. Such multiple photon emission can result either from independent dopants or recombination of multiple excitons at a solitary dopant.²⁸ In some cases, appearance of multiple PL emission peaks in low T (4 K) spectra allows us to attribute multiple photon emission to two independent dopants (Fig. 1a and b top trace).²⁹

^aCenter for Integrated Nanotechnologies, Materials Physics and Applications Division, Los Alamos National Laboratory, New Mexico, 87545, USA.
 E-mail: htoon@lanl.gov

^bTheoretical Division, Los Alamos National Laboratory, New Mexico, 87545, USA.
 E-mail: kirill@lanl.gov

†Electronic supplementary information (ESI) available: Additional data, estimation of E11 exciton population, time gated 2nd order photon correlation spectroscopy, and theoretical model. See DOI: 10.1039/c7nr06661a

‡Present address: Center for Nanoscale Materials, Argonne National Laboratory, 9700 South Cass Avenue, Argonne, Illinois 60439, United States.

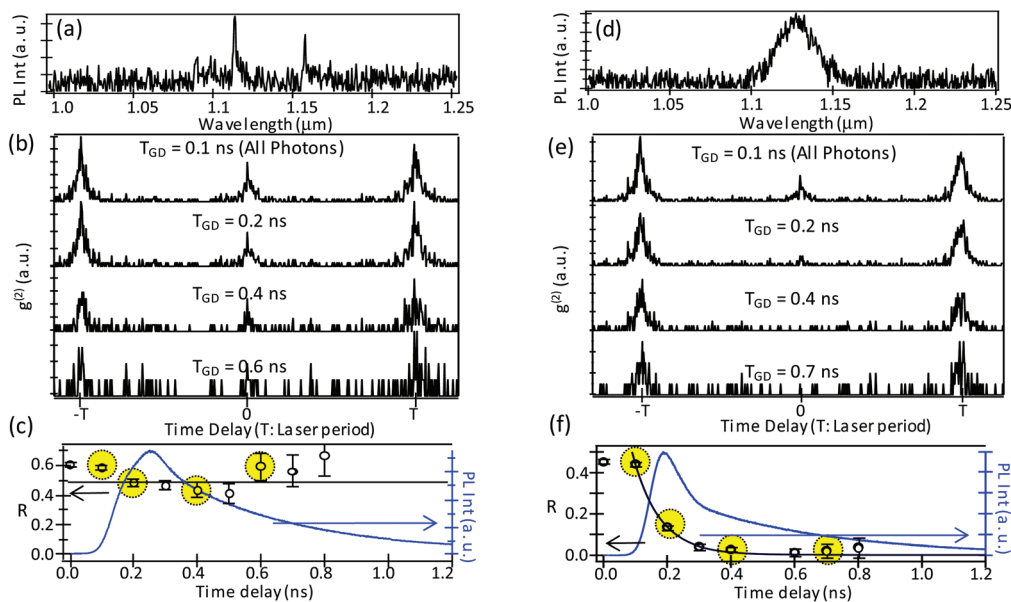


Fig. 1 PL spectra (a, d), $g^{(2)}$ trace of all the photons (top trace) and time gated $g^{(2)}$ traces extracted at the gate delay time (T_{GD}) indicated in the figures (b, e) (see ESI, Fig. 1S† for $g^{(2)}$ traces with time delay extending to 300 ns). PL decay curves (blue, right axis) and center to side peak area ratio (R) vs. T_{GD} plot (left axis) (c, f) for two doped SWCNTs. Black solid lines are guides to the eye. The data for (a–c) and (d–f) were acquired at 4 K and 200 K, respectively.

However for all the doped tubes exhibiting antibunching with $R \sim 0.2$ – 0.5 at temperatures higher than 100 K, a single dopant-related PL peak was observed, indicating a possible multi-exciton emission (Fig. 1d & e, top trace acquired at 200 K). This evidence, however, is not conclusive because at these temperatures, it is not clear whether multiple spectral lines merge into a single thermally broadened PL peak. Here, we provide experimental evidence that oxygen dopant states can allow relatively efficient multi-exciton emission. We also observe that diffusion limited, exciton–exciton annihilation process (EEA) remains an active quenching mechanism for the dopant states, as in the case of band-edge excitons.^{30–37} We develop an exciton relaxation model capable of explaining all the key experimental observations. Overall this work elucidates the rich multi-exciton processes associated with the dopant states.

Results and discussion

In this work, a two-step aqueous two-phase separation^{38–40} is used to enrich the (6,5) chirality of HiPCo (high-pressure CO conversion) grown nanotubes. The nanotubes are wrapped with sodium dodecylbenzene sulfonate (SDBS) and dispersed on glass substrates over-coated with 100 nm thick Au and SiO₂ layers.^{9,11} The undoped tubes are then covered with a 10 nm thick SiO₂ layer to achieve solid-state oxygen doping following ref. 9 & 11. The concentration of the SWCNTs is adjusted to achieve a density of 1 tube per 100 μm². The sample is then mounted in a continuous-flow liquid He cryostat and a home built microPL system equipped with two super-conducting nanowire single photon detectors was used to perform time

correlated single photon counting and Hanbury Brown and Twiss experiments. The doped SWCNTs are excited at the E₁₁ phonon side band⁴¹ at 840 nm. PL spectra of the individual ether-d and epoxide-l dopant states (d/l stand for C–O–C bond aligned perpendicular/parallel to the SWCNT axis) with 130 and 300 meV trapping energies⁵ were acquired using a linear InGaAs array detector together with a 1/8 meter spectrometer.

Fig. 1 displays representative optical data from two individual doped SWCNTs. The doped tube of Fig. 1a–c, exhibits two independent dopant sites emitting at distinct wavelengths (at 1.114 and 1.158 μm, Fig. 1a). The $g^{(2)}$ trace of all the emitted photons shows R of ~ 0.5 (Fig. 1b, top trace) consistent with the spectra.²⁹ The second doped tube (Fig. 1d–f) displays a single PL emission peak. Its $g^{(2)}$ trace, however, shows incomplete photon antibunching with R of ~ 0.44 . As discussed previously, this data alone is not sufficient to determine whether this R value results from emission of multi-excitons of a single dopant state or emission of two independent dopant states. To distinguish between these possible origins, we performed a time gated 2nd order photon-correlation experiment.^{28,42}

We applied a time gate to remove the photons detected at delay times earlier than the gate delay time (T_{GD}) and reconstructed the $g^{(2)}$ trace from the remaining photons (see ref. 28, 42 and ESI 3†). Since the two independent dopant states of the first tube should decay with similar lifetimes ($\sim 400 \pm 50$ ps),⁹ the time gate does not affect the shape of the $g^{(2)}$ function apart from reducing the signal to noise ratio as demonstrated by the three bottom $g^{(2)}$ traces in Fig. 1b. On the other hand, in the case of emission from multi-excitons of a single dopant state, application of a time gate will preferentially remove the photons of multi-exciton states because

their emission generally precedes that of single excitons due to their much shorter lifetimes.^{19,20} The R values of the reconstructed time gated $g^{(2)}$ traces, as a result, should decrease with an increase of T_{GD} . The $g^{(2)}$ traces extracted at a T_{GD} longer than the multi-exciton lifetime should show complete antibunching, as all the photons of multi-excitons are removed.^{28,42} This behavior can be observed clearly in the time gated $g^{(2)}$ traces of the 2nd tube (Fig. 1e, bottom 3 traces). This analysis therefore provides solid evidence that the central peak of the top $g^{(2)}$ trace of Fig. 1e arises from detection of two photons emitted in sequence by the multi-excitons of a single dopant state. Furthermore, because R has been shown to provide a measure of multi-excitonic emission efficiency relative to that of a single exciton state (*i.e.* $R \rightarrow QY_{MX}/QY_{1X}$),^{43,44} we can estimate the quantum yield of the multi-exciton states to be $\sim 44\%$ of the single exciton states for the tube shown in Fig. 1e.

A plot of R vs. T_{GD} (Fig. 1f data points) also shows that incomplete photon antibunching exists only at early time delays where the fast decay component dominates (Fig. 1f, blue curve). This fast component can therefore be attributed to the decay of multi-excitons. We performed pump power dependent lifetime measurements to gain further insight on decay dynamics of these multi-excitons. Fig. 2 displays the data from 2 representative single dopant sites (note: the data of Fig. 2a–c

are acquired from the same dopant site as Fig. 1d–f). The pump-dependent decay curves of Fig. 2a and the plot of average lifetime vs. pump power (Fig. 2b, red data points) show that for low pump powers up to 20 μW , the PL decay is single exponential, with the average lifetime remaining constant at ~ 200 ps. A fast component with a lifetime of ~ 50 ps (close to instrument response) emerged at higher pump powers (curves 3 & 4 of Fig. 2a) and the average lifetime decreases. The lifetimes of both fast and slow components, however, stay essentially constant for all pump powers. PL intensity increases with pump power up to 10 μW and saturates at 20 μW (where the fast decay component starts to emerge), and then decreases at the highest pump power (the last data point). PL was observed to be reduced significantly when the pump power was decreased back to 3 μW after reaching the highest pump power of 1000 μW (black triangle of Fig. 2b). The corresponding PL decay curve (curve 5) mostly recovers to that obtained before the intensity sweep (curve 1). The dopant sites of Fig. 2c and d behave similarly, except that the fast decay components rise to more prominent levels and the PL intensity roll-off happens at a much lower pump power than in the previous case (~ 5 μW). Finally, a very strong fast decay component, together with quenching of PL, is observed in the decay when the pump power is reduced back to <10 μW after the ramp to the 1000 μW maximum.

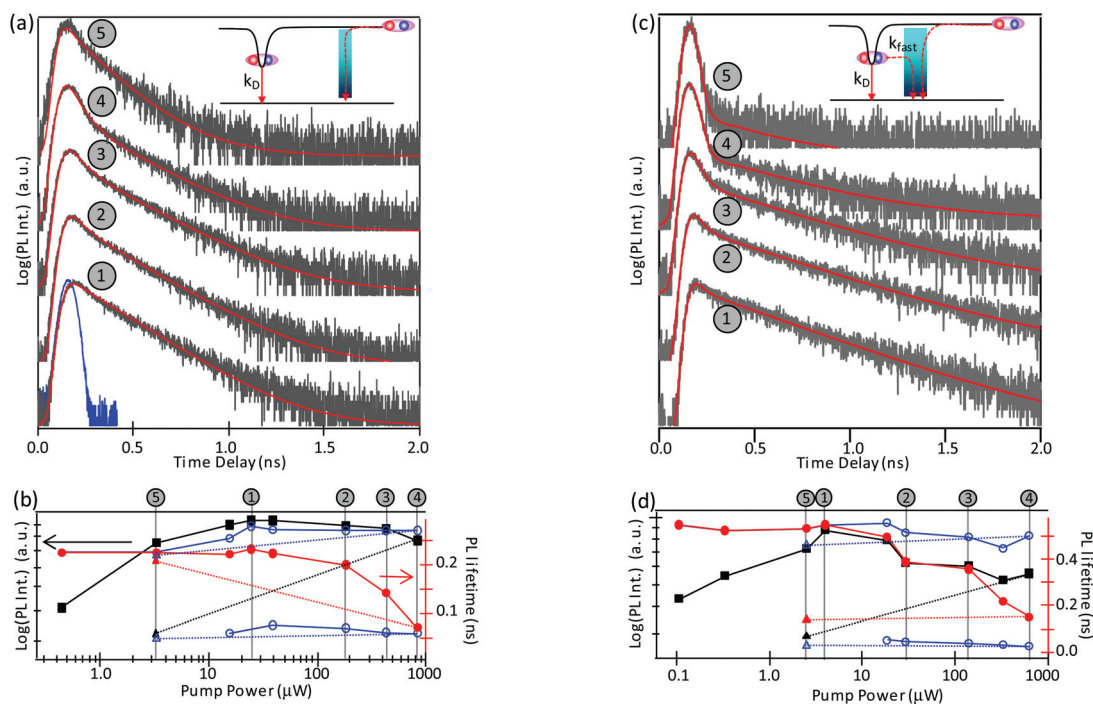


Fig. 2 (a, c) Pump dependent PL decay (gray) and curves fitted with bi-exponential function, $I(t) = A_1e^{-t/\tau_1} + A_2e^{-t/\tau_2}$ (red) of two different individual dopant sites. Instrument response function is shown in (a) as blue curve. Insets: Two mechanisms responsible for irreversible changes in intensity and/or lifetime (see text). (b, d) log–log plot of PL intensity vs. pump power (black squares), semi-log plot of fast/slow PL lifetimes of bi-exponential fits (blue circles) and averaged lifetime, $\tau_A = (A_1\tau_1^2 + A_2\tau_2^2)/(A_1\tau_1 + A_2\tau_2)$, (red circles) for the same two individual dopant sites. Triangle data points represent the PL intensity (black) and lifetimes (red: average, blue: long and short components) measured after the pump power is reduced back from the maximum. Data points for the decay curves shown in (a) & (b) are marked 1–5. All the data are acquired at 200 K. The data of a & b were measured from the same dopant site as the data of Fig. 1d–f.

To provide a qualitative explanation for our key observations, we developed a kinetic model describing the trapping, recombination and EEA processes of excitons that are initially pumped into the E_{11} band of doped SWCNTs. The model is based on the picture of various single-exciton processes (diffusion along a SWCNT, quenching, trapping) and EEA developed in ref. 45–48. In this model, described in detail in ESI 4,† exciton trapping by each of m dopants, EEA of two free E_{11} excitons, and EEA of a free exciton and a trapped exciton are assumed to be diffusion-limited processes with time-independent rate constants of k_t ,⁴⁶ k_A ,⁴⁹ and αk_A , respectively, where α is a coefficient of the order of one.⁵⁰ In the absence of dopant sites, a free exciton decays with a rate constant, k , which is determined by diffusion-limited quenching.⁴⁶ The trapped exciton recombines with a rate constant k_D .

This model can be cast in the form of a system of master equations, which can be solved analytically to yield long and cumbersome expressions (see ESI 4†). Assuming that $k_D \ll k$, k_t , k_A , these expressions can be simplified to yield

$$R(T_{GD}) \cong \frac{k_F}{k_F + \alpha k_A - k_t} \left[\frac{m-1}{m} \frac{2k_F}{2k_F + k_A} + \frac{2k_D}{k_F + (1-\alpha)k_A + k_t} e^{-(k_F + \alpha k_A - k_t)T_{GD}} \right] \quad (1)$$

where $k_F = k + mk_t$ is the inverse lifetime of an isolated free exciton in the presence of m dopant sites. When $m > 1$, the first term in square brackets of eqn (1) dominates as $k_F \gg k_D$. This results in T_{GD} -independent $R(T_{GD})$, which is in agreement with what is observed in Fig. 1c.

When $m = 1$, the first term vanishes and $R(T_{GD})$ decays rapidly with a lifetime of $\tau = (k + \alpha k_A)^{-1}$. This behavior, which is observed in Fig. 1f, can be understood as the detection of two photons from the successive radiative recombination of two trapped excitons. Since only one dopant site is present ($m = 1$), one of the two excitons has to be trapped and recombines radiatively before the second free exciton approaches the dopant site, otherwise they undergo EEA with no subsequent contribution to the photon correlation signal. The relative probability of such a process, given by a pre-exponent of the second term in eqn (1), is low because the slow recombination of a trapped exciton (k_D) has to compete with the fast diffusion-limited quenching (k) and EEA (αk_A). The rate constant of decay of a state that consists of one free and one trapped exciton is $k + \alpha k_A + k_D$, which, again assuming small k_D , produces lifetime τ obtained above.

The same solution of master equations can also be used to derive the expression for the PL intensity decay as (ESI 4†)

$$I(t) = p_1 I_1(t) + \tilde{p}_2 I_2(t), \quad (2)$$

$$I_1(t) \approx Q_D k_D A_1 e^{-k_D t}, \quad (3)$$

$$I_2(t) \approx Q_D k_D [A_2 e^{-k_D t} + B_2 e^{-(k_F + \alpha k_A - k_t)t}], \quad (4)$$

where p_1 (\tilde{p}_2) is the Poissonian probability of excitation of 1 (≥ 2) free exciton(s), and I_1 (I_2) is the respective PL intensity. The PL quantum yield of a trapped exciton is denoted by Q_D . The

coefficients A_1 , A_2 , and B_2 are very complex functions of decay constants and can be simplified to the expressions given in eqn (S12–S14) in ESI 4.† The effective rate constant $k_F + \alpha k_A - k_t$ of I_2 is similar in magnitude to diffusion-limited rate constants k , k_t , k_A and much larger than k_D . It therefore represents the fast decay component observed in the experiment (Fig. 2). The exciton population threshold required for the emergence of fast decay components can be estimated from the condition that the prefactor of the fast decay component becomes comparable in magnitude to that of the slow component, *i.e.*, $\tilde{p}_2 B_2 \sim p_1 A_1 + \tilde{p}_2 A_2$. Our analysis of this condition (see ESI 4† for details) reveals that the fast component can arise only at very high average exciton population ($f > 10$). This result is consistent with our observation that the fast decay component emerges only at excitation powers $> 20 \mu\text{W}$ corresponding to $f > 20$ excitons (Fig. 2) whereas the PL intensity saturation occurs at much lower power corresponding to $f \sim 1$.

This fast PL decay component can be understood within our model (eqn (2)) as the shortening of the effective lifetime of a trapped exciton due to arrival of the second exciton that subsequently induces the EEA process. Since EEA, as well as quenching and trapping of a free exciton, are diffusion-limited processes, they are expected to have similar time constants. Our model therefore explains why both the fast component of the PL decay of trapped excitons, observed in this work, and the decay of the free E_{11} excitons in a doped SWCNT^{9,46} are characterized with very similar (50–75 ps) time constants. Furthermore, the model predicts the time constants of the fast PL decay component and that of $R(T_{GD})$ at $m = 1$ to be exactly the same, which is observed experimentally.

The introduced model describes the emergence of the fast PL decay component at high pump fluences as a completely reversible process. The experiment, however, shows that while the emergence of the fast component is reversible in the case of Fig. 2a, it is irreversible in the case of Fig. 2c. The quenching of the PL intensity is irreversible in both cases. These irreversible changes suggest that photo-degradation under high intensity laser excitation competes with the EEA process. We suggest that in the case of Fig. 2a, strong laser irradiation introduces quenching sites (blue column in the inset of Fig. 2a) that compete with dopants in trapping free excitons. As a result, the probability of trapping of free excitons is reduced permanently and causes irreversible PL quenching. The average PL lifetime of the dopant state, however, can return to its original value as the contribution of EEA processes is reduced at lower pump powers. Within the model, this situation is described by the effective increase of rate constant k that describes the process of non-radiative quenching of excitons.

We further speculate that Fig. 2c corresponds to the scenario where a quenching site is introduced very close to the dopant (inset of Fig. 2c), so that it allows non-radiative decay of trapped excitons at a rate much faster than k_D . Both PL intensity and decay, as a result become irreversible. Within the model this effect can be simulated by the effective increase of both k and k_D rate constants. Observation of PL intensity fluctuation

tuations at high pump power⁹ suggests that the photo-induced quenching sites can switch between on and off states randomly. Such random on/off switching in the case of Fig. 2c can give rise to bi-exponential PL decay, as the decay curves were averaged over many on/off cycles.

Conclusions

In summary, using a kinetic model, we successfully explain key experimental findings, namely, the decay of $g^{(2)}(0)$ with T_{GD} and the emergence of a fast PL decay component at high pump fluences, as the direct consequence of a single dopant site emitting a pair of photons *via* successive trapping and recombination of two excitons. More quantitative usage of the model requires assigning specific values to all the rate constants, which constitutes future research. These findings show that the multi-exciton processes of the doped nanotubes are rich and exciting areas to be explored for potential applications in lasing and entangled photon generation.

Conflicts of interest

There are no conflicts to declare.

Acknowledgements

This work was conducted at the Center for Integrated Nanotechnologies, a U.S. Department of Energy, Office of Basic Energy Sciences user facility and supported by Los Alamos National Laboratory Directed Research and Development Funds.

Notes and references

- S. Ghosh, S. M. Bachilo, R. A. Simonette, K. M. Beckingham and R. B. Weisman, *Science*, 2010, **330**, 1656.
- R. Matsunaga, K. Matsuda and Y. Kanemitsu, *Phys. Rev. Lett.*, 2011, **106**, 037404.
- T. Shiraki, T. Shiraishi, G. Juhász and N. Nakashima, *Sci. Rep.*, 2016, **6**, 28393.
- H. Kwon, A. o. Furmanchuk, M. Kim, B. Meany, Y. Guo, G. C. Schatz and Y. Wang, *J. Am. Chem. Soc.*, 2016, **138**, 6878.
- X. Ma, L. Adamska, H. Yamaguchi, S. E. Yalcin, S. Tretiak, S. K. Doorn and H. Htoon, *ACS Nano*, 2014, **8**, 10782.
- Y. Piao, B. Meany, L. R. Powell, N. Valley, H. Kwon, G. C. Schatz and Y. Wang, *Nat. Chem.*, 2013, **5**, 840.
- Y. Miyauchi, M. Iwamura, S. Mouri, T. Kawazoe, M. Ohtsu and K. Matsuda, *Nat. Photonics*, 2013, **7**, 715.
- M. Iwamura, N. Akizuki, Y. Miyauchi, S. Mouri, J. Shaver, Z. Gao, L. Cognet, B. Lounis and K. Matsuda, *ACS Nano*, 2014, **8**, 11254.
- X. Ma, N. F. Hartmann, J. K. S. Baldwin, S. K. Doorn and H. Htoon, *Nat. Nanotechnol.*, 2015, **10**, 671.
- X. He, N. F. Hartmann, X. Ma, Y. Kim, R. Ihly, J. L. Blackburn, W. Gao, J. Kono, Y. Yomogida, A. Hirano, T. Tanaka, H. Kataura, H. Htoon and S. K. Doorn, *Nat. Photonics*, 2017, **11**, 577.
- X. Ma, J. K. Baldwin, N. F. Hartmann, S. K. Doorn and H. Htoon, *Adv. Funct. Mater.*, 2015, **25**, 6157.
- E. Gaufres, N. Izard, A. Noury, X. Le Roux, G. Rasigade, A. Beck and L. Vivien, *ACS Nano*, 2012, **6**, 3813.
- S. Imamura, R. Watahiki, R. Miura, T. Shimada and Y. Kato, *Appl. Phys. Lett.*, 2013, **102**, 161102.
- S. Khasminskaya, F. Pyatkov, B. S. Flavel, W. H. Pernice and R. Krupke, *Adv. Mater.*, 2014, **26**, 3465.
- R. Miura, S. Imamura, R. Ohta, A. Ishii, X. Liu, T. Shimada, S. Iwamoto, Y. Arakawa and Y. Kato, *Nat. Commun.*, 2014, **5**, 5580.
- T. Mueller, M. Kinoshita, M. Steiner, V. Perebeinos, A. A. Bol, D. B. Farmer and P. Avouris, *Nat. Nanotechnol.*, 2010, **5**, 27.
- S. Khasminskaya, F. Pyatkov, K. Słowik, S. Ferrari, O. Kahl, V. Kovalyuk, P. Rath, A. Vetter, F. Hennrich, M. M. Kappes, G. Gol'tsman, A. Korneev, C. Rockstuhl, R. Krupke and W. H. P. Pernice, *Nat. Photonics*, 2016, **10**, 727.
- N. F. Hartmann, S. E. Yalcin, L. Adamska, E. H. Háróz, X. Ma, S. Tretiak, H. Htoon and S. K. Doorn, *Nanoscale*, 2015, **7**, 20521.
- J.-M. Caruge, Y. Chan, V. Sundar, H. Eisler and M. G. Bawendi, *Phys. Rev. B: Condens. Matter*, 2004, **70**, 085316.
- E. Dekel, D. Gershoni, E. Ehrenfreund, D. Spektor, J. Garcia and P. M. Petroff, *Phys. Rev. Lett.*, 1998, **80**, 4991.
- A. Hoegele, C. Galland, M. Winger and A. Imamoglu, *Phys. Rev. Lett.*, 2008, **100**, 217401.
- M. S. Hofmann, J. T. Glueckert, J. Noe, C. Bourjau, R. Dehmel and A. Hoegele, *Nat. Nanotechnol.*, 2013, **8**, 502.
- P. Michler, A. Imamoglu, M. D. Mason, P. J. Carson, G. F. Strouse and S. K. Buratto, *Nature*, 2000, **406**, 968.
- P. Michler, A. Kiraz, C. Becher, W. V. Schoenfeld, P. M. Petroff, L. D. Zhang, E. Hu and A. Imamoglu, *Science*, 2000, **290**, 2282.
- W. Walden-Newman, I. Sarpkaya and S. Strauf, *Nano Lett.*, 2012, **12**, 1934.
- A. Dousse, J. Suffczynski, A. Beveratos, O. Krebs, A. Lemaître, I. Sagnes, J. Bloch, P. Voisin and P. Senellart, *Nature*, 2010, **466**, 217.
- O. Gazzano, S. M. de Vasconcellos, C. Arnold, A. Nowak, E. Galopin, I. Sagnes, L. Lanco, A. Lemaître and P. Senellart, *Nat. Commun.*, 2013, **4**, 1425.
- B. D. Mangum, Y. Ghosh, J. A. Hollingsworth and H. Htoon, *Opt. Express*, 2013, **21**, 4713.
- Normalized center peak area R of the $g^{(2)}$ of m independent emitter is given by $R = 1 - 1/m$.
- D. M. Harrah, J. R. Schneck, A. A. Green, M. C. Hersam, L. D. Ziegler and A. K. Swan, *ACS Nano*, 2011, **5**, 9898.

- 31 L. Huang and T. D. Krauss, *Phys. Rev. Lett.*, 2006, **96**, 057407.
- 32 Y.-Z. Ma, L. Valkunas, S. L. Dexheimer, S. M. Bachilo and G. R. Fleming, *Phys. Rev. Lett.*, 2005, **94**, 157402.
- 33 Y. Murakami and J. Kono, *Phys. Rev. Lett.*, 2009, **102**, 037401.
- 34 L. Valkunas, Y.-Z. Ma and G. R. Fleming, *Phys. Rev. B: Condens. Matter*, 2006, **73**, 115432.
- 35 Y.-F. Xiao, T. Q. Nhan, M. W. B. Wilson and J. M. Fraser, *Phys. Rev. Lett.*, 2010, **104**, 017401.
- 36 B. Yuma, S. Berciaud, J. Besbas, J. Shaver, S. Santos, S. Ghosh, R. B. Weisman, L. Cognet, M. Gallart, M. Ziegler, B. Hoenerlage, B. Lounis and P. Gilliot, *Phys. Rev. B: Condens. Matter*, 2013, **87**, 205412.
- 37 A. Hagen, M. Steiner, M. B. Raschke, C. Lienau, T. Hertel, H. Qian, A. J. Meixner and A. Hartschuh, *Phys. Rev. Lett.*, 2005, **95**, 197401.
- 38 J. A. Fagan, C. Y. Khripin, C. A. Silvera Batista, J. R. Simpson, E. H. Háróz, A. R. Hight Walker and M. Zheng, *Adv. Mater.*, 2014, **26**, 2800.
- 39 C. Y. Khripin, J. A. Fagan and M. Zheng, *J. Am. Chem. Soc.*, 2013, **135**, 6822.
- 40 N. K. Subbaiyan, S. Cambré, A. N. G. Parra-Vasquez, E. H. Háróz, S. K. Doorn and J. G. Duque, *ACS Nano*, 2014, **8**, 1619.
- 41 O. N. Torrens, M. Zheng and J. M. Kikkawa, *Phys. Rev. Lett.*, 2008, **101**, 157401.
- 42 F. Wang, N. S. Karan, H. M. Nguyen, Y. Ghosh, C. J. Sheehan, J. A. Hollingsworth and H. Htoon, *Small*, 2015, **11**, 5028.
- 43 G. Nair, J. Zhao and M. G. Bawendi, *Nano Lett.*, 2011, **11**, 1136.
- 44 Y. S. Park, A. V. Malko, J. Vela, Y. Chen, Y. Ghosh, F. Garcia-Santamaria, J. A. Hollingsworth, V. I. Klimov and H. Htoon, *Phys. Rev. Lett.*, 2011, **106**, 187401.
- 45 T. Hertel, S. Himmelein, T. Ackermann, D. Stich and J. Crochet, *ACS Nano*, 2010, **4**, 7161.
- 46 N. F. Hartmann, K. A. Velizhanin, E. H. Haroz, M. Kim, X. Ma, Y. Wang, H. Htoon and S. K. Doorn, *ACS Nano*, 2016, **10**, 8355.
- 47 J. J. Crochet, J. G. Duque, J. H. Werner, B. Lounis, L. Cognet and S. K. Doorn, *Nano Lett.*, 2012, **12**, 5091.
- 48 X. Ma, O. Roslyak, J. G. Duque, X. Pang, S. K. Doorn, A. Piryatinski, D. H. Dunlap and H. Htoon, *Phys. Rev. Lett.*, 2015, **115**, 017401.
- 49 F. Wang, Y. Wu, M. S. Hybertsen and T. F. Heinz, *Phys. Rev. B: Condens. Matter*, 2006, **73**, 245424.
- 50 M. Kim, L. Adamska, N. F. Hartmann, H. Kwon, J. Liu, K. A. Velizhanin, Y. Piao, L. R. Powell, B. Meany, S. K. Doorn, S. Tretiak and Y. Wang, *J. Phys. Chem. C*, 2016, **120**, 11268.